

Shielding Considerations for Transient Magnetic Fields Produced by a Pulsed Moving Conductor System

by Alex E. Zielinski, Ira Kohlberg, John Bennett,
Calvin D. Le, and W. Jim Sarjeant

ARL-TR-2488

May 2001

Approved for public release; distribution is unlimited.

20010613 044

The findings in this report are not to be construed as an official Department of the Army position unless so designated by other authorized documents.

Citation of manufacturer's or trade names does not constitute an official endorsement or approval of the use thereof.

Destroy this report when it is no longer needed. Do not return it to the originator.

Army Research Laboratory

Aberdeen Proving Ground, MD 21005-5066

ARL-TR-2488

May 2001

Shielding Considerations for Transient Magnetic Fields Produced by a Pulsed Moving Conductor System

Alex E. Zielinski

Weapons and Materials Research Directorate, ARL

Ira Kohlberg

Kohlberg Associates Inc.

John Bennett

U.S. Army Tank-automotive and Armaments Command-U.S. Army Armament
Research, Development, and Engineering Center

Calvin D. Le

Sensors and Electronic Devices Directorate, ARL

W. Jim Sarjeant

University of Buffalo, SUNY

Abstract

A model was developed for determining the space and time behavior of the magnetic field external to a system of conductors. A moving conductor is in relative close proximity to a stationary conductor that provides the source current. An additional conductor attenuates the environmental field. The space and time periodicity of the field are related to the parameters of the system. A numerical example predicts the magnitude of the magnetic field as a function of distance from the stationary conductor. Initial shielding considerations for mitigating the environmental effects produced by this class of emerging technologies were developed. The assessment indicates that conventional engineering design, based on the principles of electromagnetic compatibility (EMC), can reduce the magnetic fields to levels consistent with the notional requirements of electric combat vehicles.

Acknowledgments

A sincere thanks is extended to Dr. John Powell and Mr. Miguel DelGuercio, U.S. Army Research Laboratory (ARL), for performing a concise and thorough technical review of the manuscript.

INTENTIONALLY LEFT BLANK.

Contents

Acknowledgments	iii
List of Figures	vii
List of Tables	ix
1. Introduction	1
2. Theoretical Considerations	2
2.1 Model Formalism	2
2.2 Numerical Results	6
3. Environmental Shield Design	8
4. Summary and Conclusions	12
5. References	13
Distribution List	15
Report Documentation Page	19

INTENTIONALLY LEFT BLANK.

List of Figures

Figure 1. Source current elements and moving conductor.	2
Figure 2. Geometric considerations for determining the magnetic field produced by a moving conductor and environmental shield system.	3
Figure 3. Normalized source current as a function of environmental shield location.	7
Figure 4. Magnetic field as a function of dimensionless distance (η).	8
Figure 5. Measured magnetic induction field as a function of time [9].	10
Figure 6. Illustration of multilayer shield model.	10
Figure 7. Attenuated induction field as a function of environmental shield thickness.	11

INTENTIONALLY LEFT BLANK.

List of Tables

Table 1. Assumed values for numerical calculation.	7
Table 2. Fitting constants for 0.25-mm-thick shield materials [9].	10

INTENTIONALLY LEFT BLANK.

1. Introduction

Over the years, there has been continued interest in developing pulsed-power energy sources and accelerators based on the processes of transient magnetic field exclusion and diffusion. An essential feature common to these devices involves a stationary source current and induced currents (i.e., eddy currents) in a moving finite conductivity conductor. The source and eddy currents produce magnetic fields that have a characteristic magnitude and frequency external to their geometry. Applications utilizing this process can be found in the electromagnetic braking of large electromechanical systems [1, 2] and in generating high electrical power pulses [3-5].

As these electrical devices mature into components for military systems, the electromagnetic compatibility (EMC) issues that arise from the environmental electric and magnetic fields they generate must be considered. Environmental fields are those fields created in spatial locations that are not especially close to the source and are concurrently located in close proximity to a receptor of those fields; electronic equipment and humans are two examples. For example, environmental electromagnetic fields generated by capacitor-driven pulsed-power sources could impose EMC considerations for electromagnetic railguns [6, 7]. Superconducting electrical generators utilizing liquid metal slip rings are another example where EMC considerations influence the magnetic operating environment [8]. Fortunately, standard shielding techniques, using conducting materials, are adequate for managing magnetic fields less than 1 T [9]. For large confined fields, active shielding techniques can be more efficiently implemented [8, 9].

This report discusses the results of a system of three conductors: (1) a source, (2) a moving conductor located in close proximity, and (3) an environmental shield located some distance removed from the source. The magnetic induction field is of primary interest. In section 2, the results from a system of two conductors are reassessed [10] and extended to include a third conductor, an environmental shield. Realistic values are calculated for the field incident on a perfectly conducting shield. In section 3, the incident field is used to illustrate the design of an environmental shield with previously experimentally derived material properties [9]. Finally, in section 4, the summary and conclusions are presented.

2. Theoretical Considerations

The purpose of this section is to characterize the salient features of the environmental magnetic field generated by a moving conductor system that is produced by a spatially periodic, time varying source current characteristic of a low impedance source. Figure 1 shows a close up of the relationship between the spatially periodic source currents and a moving conductor. Previous work shows that image theory was applicable to this type of problem with further simplification resulting from assuming infinite conductivity for the moving conductor [10]. This work also shows that for velocities greater than 100 m/s and good conductivity for the moving conductor, the field contribution due to motion can be neglected.

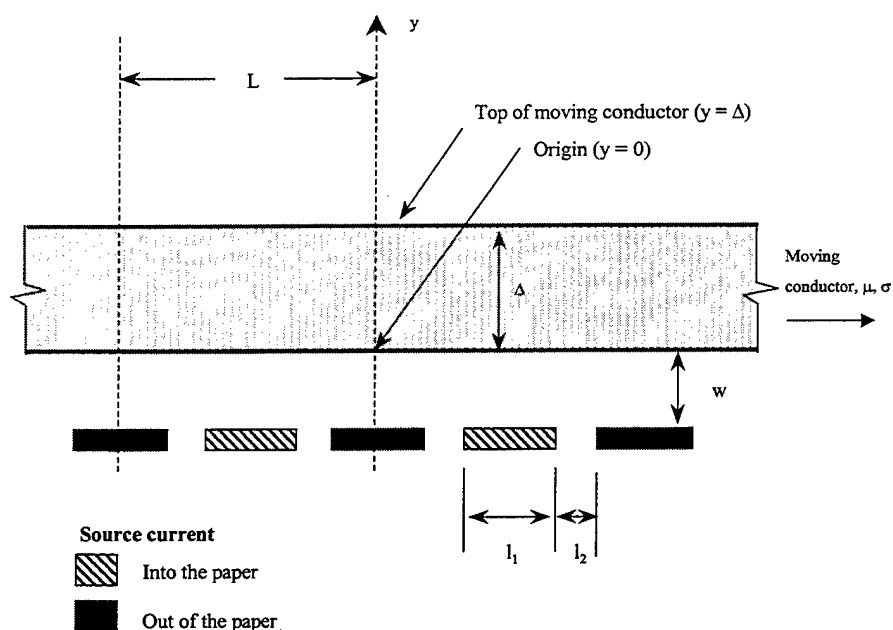
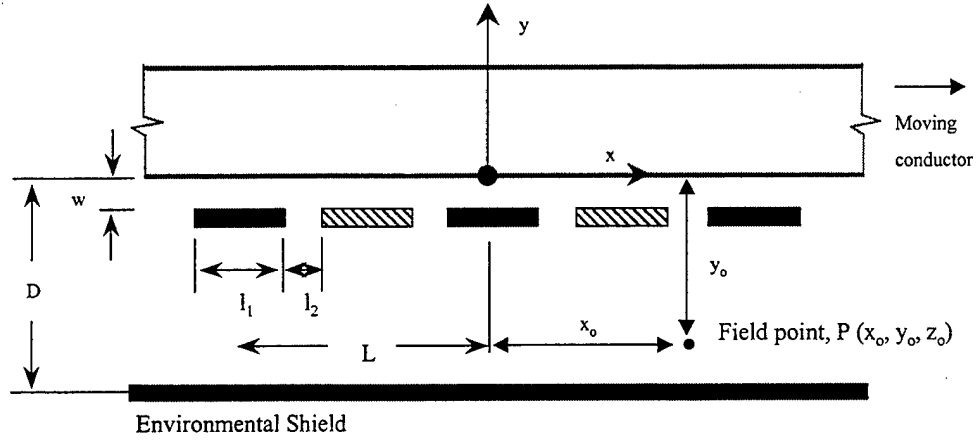


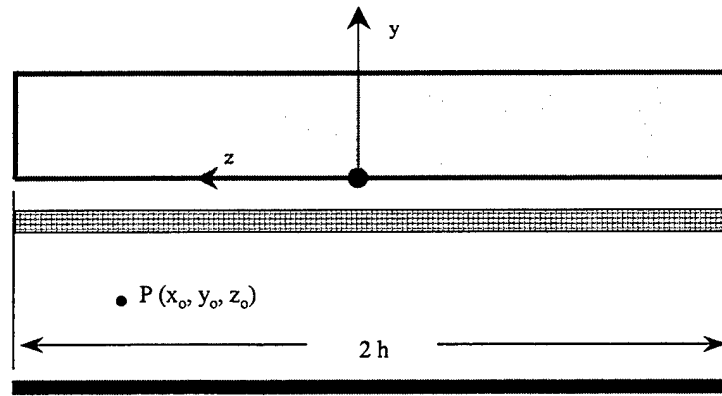
Figure 1. Source current elements and moving conductor.

2.1 Model Formalism

Figure 2 shows the geometry used for determining the ambient magnetic field in the presence of an environmental shield. It is assumed that both the moving conductor and the environmental shield have infinite conductivities and that they can be represented as an array of images. The system is assumed to be periodic and infinite in the $\pm x$ directions. Image theory permits the field in the space between the planes $y = 0$ and $y = -D$ to be computed by summing the fields due to the actual physical source and its images [10].



Front View



Side View

Figure 2. Geometric considerations for determining the magnetic field produced by a moving conductor and environmental shield system.

The discontinuous linear current density, \vec{J}_R , of the periodic distribution of source elements shown in Figure 2 can be written as $\vec{J}_R = \vec{k}J_R$. The magnitude is

$$J_R(x, t) = A_J(t) \sum_{n=1}^{\infty} a_n \cos \frac{2n\pi x}{L}, \quad (1)$$

where the characteristic length is $L = 2(l_1 + l_2)$, and the a_n 's are determined from the orthogonality properties of the Fourier series. Using the discontinuous distributions

$$J_R(x) = A_J : \frac{l_1}{2} \geq |x| \geq 0,$$

$$= 0 : \frac{l_1}{2} + l_2 \geq |x| \geq \frac{l_1}{2},$$

and

$$= -A_J : l_1 + l_2 \geq |x| \geq \frac{l_1}{2} + l_2, \quad (2)$$

where A_J is a constant;

$$a_n = \frac{2}{n\pi} (1 - \cos n\pi) \sin \frac{n\pi l_1}{L}. \quad (3)$$

The environmental magnetic field is computed for the region below the source conductors—for field points satisfying the condition $y_o < -w$. The starting point for the calculation of the magnetic field at position

$$\vec{r}_o = \vec{i}x_o + \vec{j}y_o + \vec{k}z_o \quad (4)$$

is the two-dimensional form of the Biot-Savart law given by

$$\vec{B}(\vec{r}_o) = \frac{\mu_o}{4\pi} \iint \frac{\vec{J}(\vec{r}) \times (\vec{r}_o - \vec{r})}{|\vec{r}_o - \vec{r}|^3} dx dz. \quad (5)$$

When only the real source and its image are considered, the magnetic field at \vec{r}_o is given by

$$\vec{B}(\vec{r}_o) = \vec{B}_R(\vec{r}_o) + \vec{B}_I(\vec{r}_o), \quad (6)$$

where \vec{B}_R and \vec{B}_I are the contributions from the real and image sources, respectively, and \vec{B}_R is given by

$$\vec{B}_R = \frac{\mu_o}{4\pi} \int_{-\infty}^{+\infty} \int_{-h}^{+h} \frac{\vec{k} dz \times \vec{r}_R}{|\vec{r}_R|^3} J_R(x) dx. \quad (7)$$

The integration over x extends from $-\infty$ to $+\infty$, the integration over z extends from $-h$ to $+h$, and

$$\vec{r}_R = \vec{i}(x_o - x) + \vec{j}(y_o + w) + \vec{k}(z_o - z). \quad (8)$$

The foregoing expression simplifies when the observation point is located at the intersection of the midplanes $x_o = 0$ and $z_o = 0$. With respect to z in equation 7, the integration then yields for the contribution due to the source current

$$\bar{B}_R = -\vec{i} \frac{\mu_o}{4\pi} (y_o + w) \int_{-\infty}^{+\infty} J_R \frac{2h}{(x^2 + (y_o + w)^2)(h^2 + x^2 + (y_o + w)^2)^{1/2}} dx. \quad (9)$$

It is simplified when the foregoing equations are cast in dimensionless form by introducing the variables

$$\rho = \frac{x}{L} \quad (10)$$

and

$$\eta = \frac{y_o + w}{L} \quad (11)$$

and selecting a specific value for h . For convenience, a value of $h = L$ is used. Inserting equation 1 into equation 9 and dropping the vector notation gives

$$B_R = -\frac{\mu_o}{4\pi} A_J \sum_{n=1}^{n=\infty} a_n P_n(\eta), \quad (12)$$

where

$$P_n = 4\eta \int_0^{\infty} \frac{\cos 2n\pi\rho}{(\eta^2 + \rho^2)(1 + \eta^2 + \rho^2)^{1/2}} d\rho \approx 2\pi e^{-2\pi n\eta} \quad (13)$$

valid for $\eta > 0.025$.

But there is also

$$P_n(-\eta) = -P_n(\eta), \quad (14)$$

which is relevant since y_o is negative.

The development of the magnetic field due to the image current in the moving conductor is similar [10];

$$B_I = \frac{\mu_o}{4\pi} A_J \sum_{n=1}^{n=\infty} a_n P_n(\eta - \frac{2w}{L}). \quad (15)$$

The net magnetic field for the two conductor system is given as

$$B_{net} = B_R(\eta) - B_R(\eta - \frac{2w}{L}). \quad (16)$$

The total magnetic field, B_{tot} , for the three conductor system in terms of the source contribution, is computed from the formalism of equations 12-14. Image currents in the shield now contribute to the total field and can be expressed as an infinite series. The argument η of B_R is replaced by $(\eta + \frac{2mD}{L})$ and

$(\eta - \frac{2w}{L} + \frac{2mD}{L})$ for all integer values of m , to reflect the contribution due to the image currents. Thus,

$$B_{tot} = \sum_{m=-\infty}^{m=+\infty} [B_R(\eta + \frac{2mD}{L}) - B_R(\eta - \frac{2w}{L} + \frac{2mD}{L})]. \quad (17)$$

The negative sign in front of the second term on the right reflects the fact that these image currents are the negative of the real current.

2.2 Numerical Results

The purpose of this section is to obtain numerical estimates of the magnetic flux density as a function of vertical distance from the source conductor system for a particular set of parameters.

For an environmental shield located some distance from the source, the eddy currents induced in the shield have very little influence on the flux density generated by the current source. However, as the shield is positioned relatively close to the source current, the flux density at the source is decreased because of the eddy currents that produce a magnetic field in the vicinity of the source in opposition to the field generated by the source. Generally, a large flux density in the air gap is desired to maintain good coupling between the source and moving conductor. If the application is electromagnetic braking, then the distance required to reduce the conductor velocity to zero will be increased because of the smaller flux density. If the application is a power source, then the generated voltage will be less, again due to the reduced flux density.

As an example, consider $l_1 = 33$ mm, $l_2 = 10$ mm, and $L = h = 50$ mm to describe the conductor geometry. In Figure 3, the source current (normalized to the current required to maintain the same air gap density without an environmental shield) is plotted as a function of the location of the environmental shield. The distance is normalized to the characteristic length. The plot includes three different values for the air gap (w). For a small air gap, as is required for efficient electromagnetic coupling, the shield's location has a negligible effect on increasing the source current. For larger air gaps, generally used because of structural requirements on the conductors, the increase in source current is somewhat larger.

For example, a 10-mm air gap and an environmental shield located 20 mm from the source yields an 8% increase in the source current or, alternatively, a 16% increase in ohmic losses, an appreciable effect on the conductor system, configured as either a load or generator.

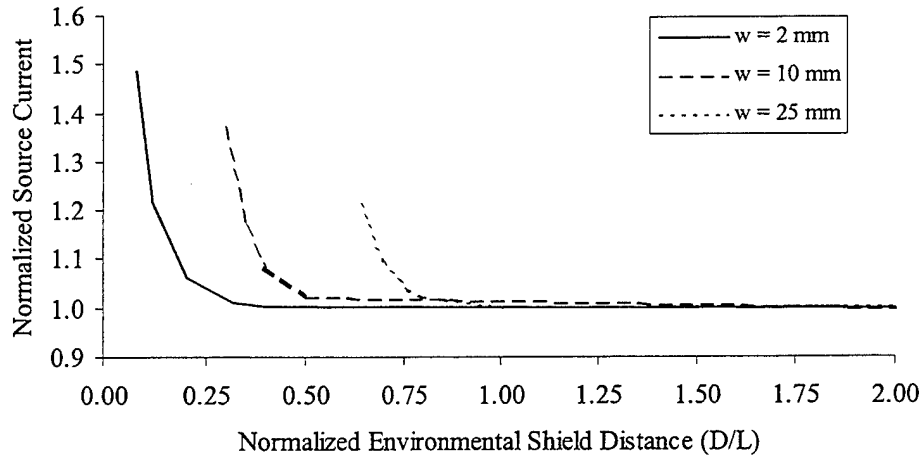


Figure 3. Normalized source current as a function of environmental shield location.

For evaluation of a realistic shield, values to describe the conductor geometry are listed in Table 1. The shield is placed far enough away from the source that it does not affect the flux density produced in the air gap; yet, it is close enough to the source to demand reasonable attenuation from an environmental shield. The shield located at $D=200$ mm ($D/L=0.29$) meets this requirement.

Using the numbers provided in Table 1 and noting from equation 3 that $a_n=0$ for $n = \text{even numbers}$, $a_1 = 1.15$ and $a_3 = -0.094$. Subsequent values of a_n are negligible. Moreover, when a_1 and a_3 are combined with the evaluation of equation 13, the third harmonic is less than 10% of the first harmonic. Hence, with very good approximation, reasonably accurate results are developed for $n=1$. Similarly, m in equation 17 is taken from -2 to $+2$.

Table 1. Assumed values for numerical calculation.

Conductor Width	l_1 (mm)	250
Conductor Spacing	l_2 (mm)	100
Characteristic Length	L (m)	0.7
Air Gap	w (mm)	5
Conductor Depth	h (m)	L
Peak Source Current	I_o (MA)	1
Shield Location	D (mm)	200

The magnetic field is computed in Figure 4 as a function of distance from the source. At the source, the induction field is roughly 5 T. The figure also shows the magnetic field for the case where no environmental shield is included. In both cases, the magnetic field decays as a function of increasing distance from the source. The linear rate of decay is roughly 1 T/m. However, the field is slightly larger in the region of space between the source and shield for the case with an environmental shield. The field incident on the shield is 0.092 T, which is not an exorbitant quantity, but it is sufficient to cause some EMC issues [9]. By definition, the field on the opposite side of the perfectly conducting shield is zero.

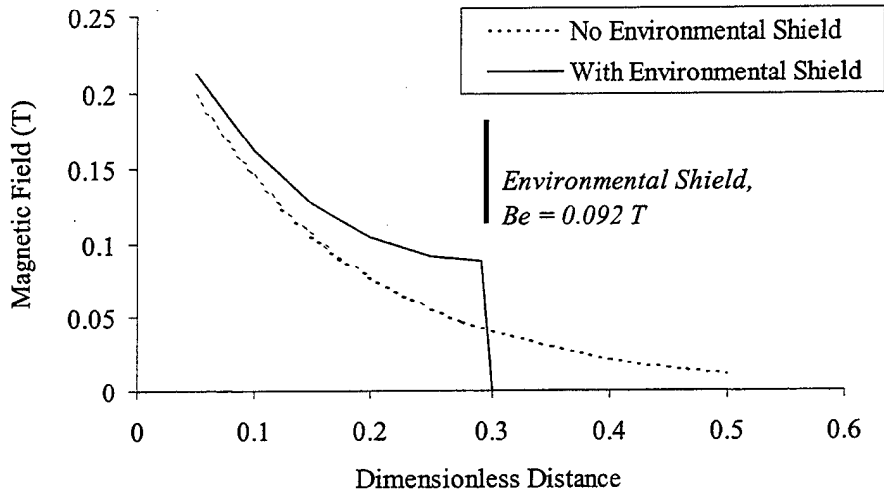


Figure 4. Magnetic field as a function of dimensionless distance (η).

3. Environmental Shield Design

In the previous section, the environmental field in the region of space beyond the perfectly conducting shield was zero. In this section, the details of a finite conductivity shield are discussed. Experimentally obtained data characterizing the shield materials are used to quantify the design [9].

For a realistic environmental shield, the field beyond the shield will not be zero, but rather a small value. Small is a subjective term, but in this case it is considered several orders of magnitude below the flux density generated in the air gap. For EMC considerations, the susceptibility of electronic components is evaluated as a function of the environmental field. This evaluation is complex

and very specific to the types of electronic components and their relative location and orientation to the source field. In the case of superconducting electrical machinery, the environmental magnetic field can cause unacceptable viscous and ohmic losses in the liquid-metal current collection system [8]. Sufficiently attenuating the field can reduce the losses to acceptable levels. However, to illustrate the current design analysis, a more simple exposure guideline, as determined by the American Conference of Governmental Industrial Hygienists (ACGIH), is used. The ACGIH threshold limit value (TLV) for exposure to a cyclical magnetic field [11] is given by

$$B_{TLV} = \frac{0.06}{f}, \quad (18)$$

where f is the frequency of oscillation for the magnetic field and B_{TLV} is in Tesla.

Numerous nomenclature are used to describe the attenuation of magnetic fields. In this study, experimental results are adapted from the literature that describe the attenuation as the ratio of the peak incident field (B_e) to the peak attenuated field (B_i), and magnetic shielding effectiveness (MSE) is described as a function of different materials and thicknesses [9]. Typically, the MSE is complex; however, only the magnitudes are considered. For magnetic materials, MSE is a function of the induction field since the permeability depends on the induction field.

Shown in Figure 5 are the exposure and attenuated fields for an 8-layer shield (2-mm total thickness) constructed from TI-Shield. The exposure field has a peak of 0.11 T at a time of 0.46 ms, which corresponds to a frequency of 543 Hz. While the magnitude of the attenuated field is reduced to 0.06 T, the rise to peak increases to 0.82 ms. The rate of decay is slightly smaller for the attenuated field than it is for the exposure field. The MSE discussed thus far depends somewhat on the waveform of the incident field.

A multilayer shield model can be used to describe the experimental arrangement and is illustrated in Figure 6. Using a fit to the MSE of the form

$$MSE = ZB_o^c + 1, \quad (19)$$

where B_o is the incident field (i.e., $B_e=B_o$ for a single-layer shield). Experimental data [9] is used to ascertain the material constants (Z and c) and are listed in Table 2. For the magnetic materials, the MSE is nearly 1 at a peak induction field of roughly 0.14 T (i.e., saturation). For the copper material, the MSE is nearly constant for all field levels, and any deviation is attributable to the accuracy of the measurements and subsequent fit to the data.

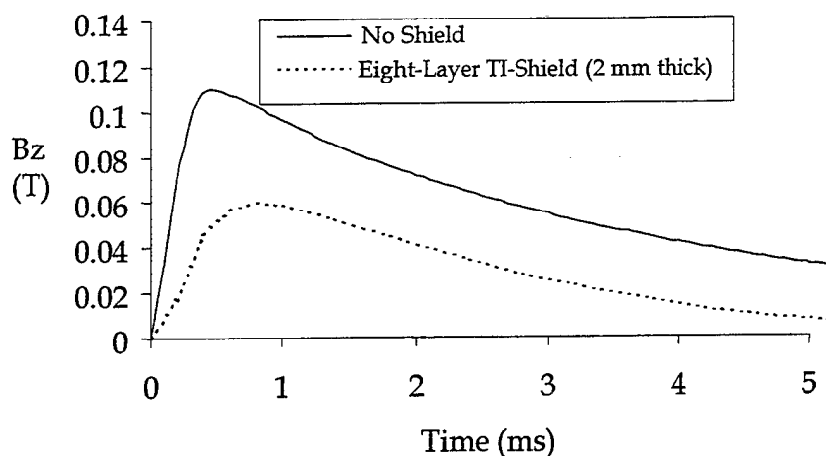


Figure 5. Measured magnetic induction field as a function of time [9].

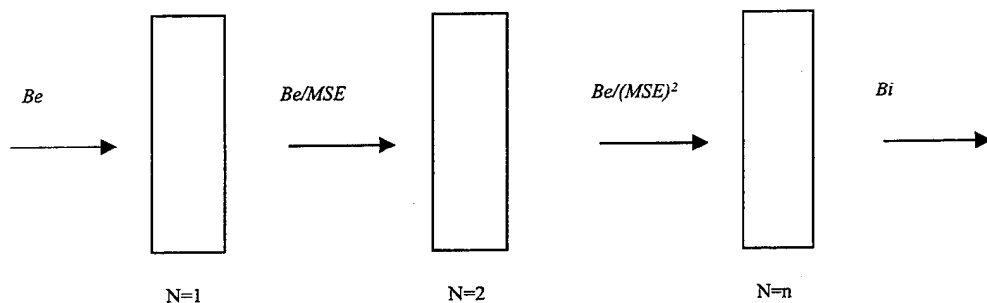


Figure 6. Illustration of multilayer shield model.

Table 2. Fitting constants for 0.25-mm-thick shield materials [9].

Material	c	Z
Copper	-0.7604	0.0065
TI-Shield	-1.4942	0.0017
M μ -Shield	-1.2401	0.0026

The geometry of the experiment and shield configuration can also affect the MSE. The constants listed in Table 2 were obtained for a cylindrical shield where a railgun was used to provide a source of pulsed magnetic field [9]. The cylinders were open at both ends and were relatively short, having a ratio of length-to-diameter of about 1.2. Additional data taken with one end of the cylinder closed increased the MSE by roughly 25%. The corrected MSE data correlate very well to a calculation for the skin depth for an incident field at the surface of a flat-plate conductor. However, no attempt was made to adjust the

constants listed in Table 2 to correspond to the environmental shield illustrated in Figure 2.

The multilayer model illustrated in Figure 6, along with the material constants listed in Table 2, was used to successfully predict the attenuated field [9]. Some disparity between theory and experiment was obtained for the number of layers greater than five. This was attributed to the outermost layers in close proximity to the rail conductors, which carried a small amount of current and thereby canceled a portion of the shielded flux. This effect was not accounted for in equation 19.

With a computation for the incident field and experimentally validated attenuation coefficients, the thickness of an environmental shield can be calculated. The attenuated magnetic field just beyond the environmental shield is shown in Figure 7 as a function of total shield thickness. The constants listed in Table 2 were used with the multilayer shield model. The incident field ($B_e = 0.092$ T) is taken from Figure 4 at the location of the environmental shield ($D = 200$ mm). For this level of incident field, there is very little difference in attenuation between the copper and magnetic materials for a total shield thickness of 5 mm. As expected, the copper shield provides a near-linear attenuation of the field as a function of shield thickness. An aluminum shield would yield similar results. The $M\mu$ -Shield material performs slightly better than the copper shield. The TI-Shield material, comprised of copper, Permalloy 49, and copper, performs even better, providing the largest attenuation for the thinnest shield.

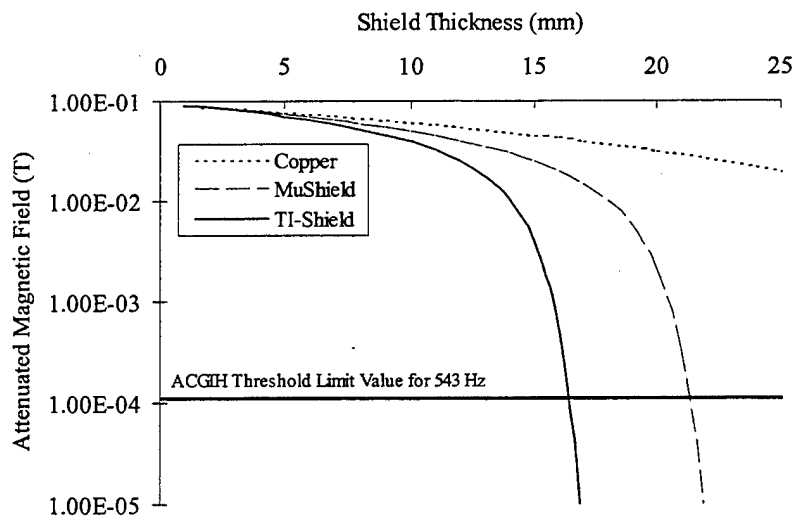


Figure 7. Attenuated induction field as a function of environmental shield thickness.

Roughly 60 dB of attenuation is provided for 15 mm of total shield thickness. Additional 20 dB increments in attenuation are easily attained for relatively insignificant increases in shield thickness greater than 15 mm. Also, the plot indicates the ACGIH TLV (~ 0.1 mT) corresponding to a frequency of 543 Hz, the fundamental frequency for the experimentally validated results [9]. The parameters listed in Table 1 correspond to a conductor moving at a velocity of 380 m/s, well within the limits of the assumption for perfect conductors. Although not indicated in the plot, the attenuated field will also decay as the distance from the shield is increased (barring the inclusion of any other source of electromagnetic radiation). Finally, the data presented in Figure 5 also suggest that the frequency of the attenuated field will be somewhat lowered, thereby complicating any additional EMC requirements.

4. Summary and Conclusions

A model has been developed for determining the space and time behavior of the magnetic field external to a system of conductors. The model includes a moving conductor in relative close proximity to a stationary (source) conductor and an environmental shield. The analysis indicates that the magnetic field has a space and time periodicity that can be related to the parameters of the conductors. Furthermore, a numerical example is presented that predicts the magnitude of the magnetic induction field as a function of distance from the stationary conductor. In this analysis, the induced currents in the environmental shield, placed in relative close proximity to the source, can reduce the flux density at the source. The corresponding increase in the source current can be appreciable (i.e., $> 25\%$) for all but the most efficiently coupled conductors (i.e., small air gap). The environmental magnetic field decays to a manageable level at distances that produce a negligible effect on the source.

A composite shield design efficiently attenuated the field produced by the conductor system to acceptable levels. The multilayer, 0.25-mm-thick TI-Shield provided 60 dB of attenuation for roughly 15 mm of total thickness. The TI-Shield can be better utilized when field levels have been reduced to less than 0.06 T. Specific exposure limits related to EMC were not available; however, the attenuated field is within the exposure guidance prescribed by ACGIH. While no attempt was made to include materials typically found on vehicles, there is no reason to suspect that existing metallic structures (i.e., steel) cannot be used to provide initial attenuation to 0.06 T.

5. References

1. Bennett J., T. Gora, P. Kemmey, and W. Kolkert. "Electromagnetic Braking of a Metallic Projectile in Flight." *IEEE Transactions on Magnetics*, vol. 21, no. 3, May 1985.
2. Doyle, M. R., D. Samuel, T. Conway, and R. Klimowski. "Electromagnetic Aircraft Launch Systems - EMALS." *IEEE Transactions on Magnetics*, vol. 31, no. 1, pp. 528-533, January 1995.
3. Summerfield, M. "Development of a Linear Piston-Type Pulse Power Electric Generator for Powering Electric Guns." *IEEE Transactions on Magnetics*, vol. 29, no. 1, January 1993.
4. Kilgore, L. A., E. Hill, and C. Flick. "A New Three Million KVA Short Circuit Generator." *IEEE Transactions (Power Apparatus and Systems)*, vol. 67, pp. 442-445, August 1963.
5. Pratap, S., and M. Driga. "Compensation in Pulsed Alternators." *IEEE Transactions on Magnetics*, vol. 35, no. 1, pp. 372-377, January 1999.
6. Kohlberg, I., C. Le, and A. Zielinski. "Predictions and Observations of Transient Electric and Magnetic Fields Generated by Electromagnetic Launch Systems." Conference Paper, XXVII International Union of Radio Science (URSI) General Assembly, Lille, France, 28 August-5 September 1996.
7. Zielinski, A. E., C. Le, J. Bennett, and I. Kohlberg. "Railgun Electric Fields: Experiment and Theory." *IEEE Transactions on Magnetics*, vol. 31, no. 1, pp. 463, January 1999.
8. Bumby, J. R. *Superconducting Rotating Electrical Machines*. Department of Engineering, University of Durham, Oxford: Clarendon Press, 1983.
9. Zielinski, A. E. "In-Bore Magnetic Field Management." ARL-TR-1914, U.S. Army Research Laboratory, Aberdeen Proving Ground, MD, March 1999.
10. Kohlberg, I., A. E. Zielinski, and C. Le. "Transient Electromagnetic Fields Produced by Pulsed Moving Conductors." ARL-TR-1931, U.S. Army Research Laboratory, Aberdeen Proving Ground, MD, April 1999.
11. Hitchcock, R. T., and R. M. Patterson. *Radio-Frequency and ELF Electromagnetic Energies: A Handbook for Health Professionals*. American Conference of Governmental Industrial Hygienists (ACGIH) Publication 9525, 1995.

INTENTIONALLY LEFT BLANK.

<u>NO. OF COPIES</u>	<u>ORGANIZATION</u>	<u>NO. OF COPIES</u>	<u>ORGANIZATION</u>
2	DEFENSE TECHNICAL INFORMATION CENTER DTIC OCA 8725 JOHN J KINGMAN RD STE 0944 FT BELVOIR VA 22060-6218	1	DIRECTOR US ARMY RESEARCH LAB AMSRL CI AI R 2800 POWDER MILL RD ADELPHI MD 20783-1197
1	HQDA DAMO FDT 400 ARMY PENTAGON WASHINGTON DC 20310-0460	3	DIRECTOR US ARMY RESEARCH LAB AMSRL CI LL 2800 POWDER MILL RD ADELPHI MD 20783-1197
1	OSD OUSD(A&T)/ODDR&E(R) DR R J TREW 3800 DEFENSE PENTAGON WASHINGTON DC 20301-3800	3	DIRECTOR US ARMY RESEARCH LAB AMSRL CI IS T 2800 POWDER MILL RD ADELPHI MD 20783-1197
1	COMMANDING GENERAL US ARMY MATERIEL CMD AMCRDA TF 5001 EISENHOWER AVE ALEXANDRIA VA 22333-0001		<u>ABERDEEN PROVING GROUND</u>
1	INST FOR ADVNCD TCHNLGY THE UNIV OF TEXAS AT AUSTIN 3925 W BRAKER LN STE 400 AUSTIN TX 78759-5316	2	DIR USARL AMSRL CI LP (BLDG 305)
1	DARPA SPECIAL PROJECTS OFFICE J CARLINI 3701 N FAIRFAX DR ARLINGTON VA 22203-1714		
1	US MILITARY ACADEMY MATH SCI CTR EXCELLENCE MADN MATH MAJ HUBER THAYER HALL WEST POINT NY 10996-1786		
1	DIRECTOR US ARMY RESEARCH LAB AMSRL D DR D SMITH 2800 POWDER MILL RD ADELPHI MD 20783-1197		

<u>NO. OF COPIES</u>	<u>ORGANIZATION</u>	<u>NO. OF COPIES</u>	<u>ORGANIZATION</u>
1	DIR FOR THE DIRECTORATE OF FORCE DEVELOPMENT US ARMY ARMOR CENTER COL E BRYLA FT KNOX KY 40121-5000	1	KAMAN ELECTROMAGNETICS CORP P MONGEAU 2 FOX RD HUDSON MA 01749
2	US ARMY RESEARCH LABORATORY C LE G MCNALLY 2800 POWDER MILL RD ADELPHI MD 20783-1145	3	LOCKHEED MARTIN N WELLS L FARRIS J NONTE PO BOX 650003 MS WT 21 DALLAS TX 75265-0003
1	US ARMY MISSILE COMMAND AMSMI RD DR MCCORKLE REDSTONE ARSENAL AL 35898-5240	1	INST FOR DEFENSE ANALYSIS I KOHLBERG 1801 N BEAUREGARD ST ALEXANDRIA VA 22311
2	US ARMY TACOM TARDEC J CHAPIN M TOURNER AMSTA TR D MS 207 WARREN MI 48397-5000	1	UNITED DEFENSE B MARINOS 1205 COLEMAN AVE SANTA CLARA CA 95050
2	US ARMY TACOM ARDEC J BENNETT D LADD FSAE GCSS TMA BLDG 354 PICATINNY ARSENAL NJ 07806-5000	1	UNIV AT BUFFALO SUNY AB J SARJEANT PO BOX 601900 BUFFALO NY 14260-1900
3	INST FOR ADVANCED TECH UNIV OF TEXAS AT AUSTIN P SULLIVAN F STEPHANI I MCNAB 3925 2 WEST BRAKER LANE SUITE 400 AUSTIN TX 78759-5316	2	UDLP B GOODELL R JOHNSON MS M170 4800 EAST RIVER RD MINNEAPOLIS MN 55421-1498
3	UNIV OF TEXAS AT AUSTIN CENTER FOR ELECT A WALLS J KITZMILLER S PRATAP PRC MAIL CODE R7000 AUSTIN TX 78712	1	UNIV OF TEXAS AT AUSTIN M DRIGA DEPT OF ECE MAIL CODE C0803 AUSTIN TX 78712
		1	SAIC G CHRYSSOMALLIS 3800 WEST 80 TH ST SUITE 1090 BLOOMINGTON MN 55431

<u>NO. OF COPIES</u>	<u>ORGANIZATION</u>	<u>NO. OF COPIES</u>	<u>ORGANIZATION</u>
1	SAIC J BATTEH 1225 JOHNSON FERRY RD SUITE 100 MARIETTA GA 30068	1	DEP DIRCTR TECHNOLOGY ID AND ANALYSIS CNTR SCIENCE AND TECH DIV INST FOR DEFENSE ANALYSES G BOEZER 1801 N BEAUREGARD ST ALEXANDRIA VA 22311-1772
1	SAIC K A JAMISON 1247 B N EGLIN PKWY SHALIMAR FL 32579		
			<u>ABERDEEN PROVING GROUND</u>
2	IAP RESEARCH INC D BAUER J BARBER 2763 CULVER AVE DAYTON OH 45429-3723	21	DIR USARL AMSRL WM E SCHMIDT AMSRL B A HORST A TANNER AMSRL WM WD J POWELL AMSRL WM B B FORCH AMSRL WM B D LYON AMSRL WM BC P PLOSTINS J GARNER V OSKAY M DELGUERCIO M BUNDY J SAHU P WEINACHT B GUIDOS A ZIELINSKI D WEBB G COOPER K SOENCKSEN S WILKERSON T ERLINE J NEWILL
1	NORTH CAROLINA STATE UNIV M BOURHAM DEPT OF NUCLEAR ENGR BOX 7909 RALEIGH NC 27695-7909		
1	MAXWELL PHYSICS INTERNATIONAL C GILMAN 2700 MERCED STREET PO BOX 5010 SAN LEANDRO CA 94577-0599		
1	PHILLIPS LABORATORY WSR C BAUM KIRTLAND AFB NM 87117		
1	CENTER FOR NAVAL ANALYSIS F BOMSE 4401 FORD AVENUE PO BOX 16268 ALEXANDRIA VA 22302-0268		
1	SPECTRAL SYNTHESIS LABS R GARDNER 6152 MANCHESTER PARK CIR ALEXANDRIA VA 22310-4957		

INTENTIONALLY LEFT BLANK.

REPORT DOCUMENTATION PAGE			Form Approved OMB No. 0704-0188
Public reporting burden for this collection of information is estimated to average 1 hour per response, including the time for reviewing instructions, searching existing data sources, gathering and maintaining the data needed, and completing and reviewing the collection of information. Send comments regarding this burden estimate or any other aspect of this collection of information, including suggestions for reducing this burden, to Washington Headquarters Services, Directorate for Information Operations and Reports, 1215 Jefferson Davis Highway, Suite 1204, Arlington, VA 22202-4302, and to the Office of Management and Budget, Paperwork Reduction Project(0704-0188), Washington, DC 20503.			
1. AGENCY USE ONLY (Leave blank)	2. REPORT DATE May 2001	3. REPORT TYPE AND DATES COVERED Final, March 1999-July 2000	
4. TITLE AND SUBTITLE Shielding Considerations for Transient Magnetic Fields Produced by a Pulsed Moving Conductor System		5. FUNDING NUMBERS AH80	
6. AUTHOR(S) Alex E. Zielinski, Ira Kohlberg,* John Bennett,† Calvin D. Le, and W. Jim Sarjeant‡			
7. PERFORMING ORGANIZATION NAME(S) AND ADDRESS(ES) U.S. Army Research Laboratory ATTN: AMSRL-WM-BC Aberdeen Proving Ground, MD 21005-5066		8. PERFORMING ORGANIZATION REPORT NUMBER ARL-TR-2488	
9. SPONSORING/MONITORING AGENCY NAMES(S) AND ADDRESS(ES)		10. SPONSORING/MONITORING AGENCY REPORT NUMBER	
11. SUPPLEMENTARY NOTES *Kohlberg Associates Inc., P.O. Box 23077, Alexandria, VA 22304; †U.S. Army Tank-automotive and Armaments Command-U.S. Army Armament Research, Development, and Engineering Center, Picatinny Arsenal, NJ 07806-5000; ‡University of Buffalo-SUNY AB, P.O. Box 601900, Buffalo, NY 14260-1900			
12a. DISTRIBUTION/AVAILABILITY STATEMENT Approved for public release; distribution is unlimited.		12b. DISTRIBUTION CODE	
13. ABSTRACT (Maximum 200 words) A model was developed for determining the space and time behavior of the magnetic field external to a system of conductors. A moving conductor is in relative close proximity to a stationary conductor that provides the source current. An additional conductor attenuates the environmental field. The space and time periodicity of the field are related to the parameters of the system. A numerical example predicts the magnitude of the magnetic field as a function of distance from the stationary conductor. Initial shielding considerations for mitigating the environmental effects produced by this class of emerging technologies were developed. The assessment indicates that conventional engineering design, based on the principles of electromagnetic compatibility (EMC), can reduce the magnetic fields to levels consistent with the notional requirements of electric combat vehicles.			
14. SUBJECT TERMS shielding, attenuation, magnetic field		15. NUMBER OF PAGES 24	
		16. PRICE CODE	
17. SECURITY CLASSIFICATION OF REPORT UNCLASSIFIED	18. SECURITY CLASSIFICATION OF THIS PAGE UNCLASSIFIED	19. SECURITY CLASSIFICATION OF ABSTRACT UNCLASSIFIED	20. LIMITATION OF ABSTRACT UL

INTENTIONALLY LEFT BLANK.

USER EVALUATION SHEET/CHANGE OF ADDRESS

This Laboratory undertakes a continuing effort to improve the quality of the reports it publishes. Your comments/answers to the items/questions below will aid us in our efforts.

1. ARL Report Number/Author ARL-TR-2488 (Zielinski) Date of Report May 2001

2. Date Report Received _____

3. Does this report satisfy a need? (Comment on purpose, related project, or other area of interest for which the report will be used.) _____

4. Specifically, how is the report being used? (Information source, design data, procedure, source of ideas, etc.) _____

5. Has the information in this report led to any quantitative savings as far as man-hours or dollars saved, operating costs avoided, or efficiencies achieved, etc? If so, please elaborate. _____

6. General Comments. What do you think should be changed to improve future reports? (Indicate changes to organization, technical content, format, etc.) _____

Organization _____
CURRENT ADDRESS Name _____ E-mail Name _____
Street or P.O. Box No. _____
City, State, Zip Code _____

7. If indicating a Change of Address or Address Correction, please provide the Current or Correct address above and the Old or Incorrect address below.

Organization _____
OLD ADDRESS Name _____
Street or P.O. Box No. _____
City, State, Zip Code _____

(Remove this sheet, fold as indicated, tape closed, and mail.)
(DO NOT STAPLE)

DEPARTMENT OF THE ARMY

OFFICIAL BUSINESS

BUSINESS REPLY MAIL
FIRST CLASS PERMIT NO 0001,APG,MD

POSTAGE WILL BE PAID BY ADDRESSEE

DIRECTOR
US ARMY RESEARCH LABORATORY
ATTN AMSRL WM BC
ABERDEEN PROVING GROUND MD 21005-5066



NO POSTAGE
NECESSARY
IF MAILED
IN THE
UNITED STATES

